Bidirectional Type III Solar Radio Burst

Yingjie Luo

2017/03/30

MorophologiesType III solar radio burst

Type III radio burst is highly related to the fast electron beams, and in dynamic spectrum it will shows the rapid frequency drift. And according to the different geometries of electron beams popagation, the dynamic spectrum will also show the different morophologies. Normally we can classify the geometries of beam popagation into 4 condition(by P.A. Robison,2000).

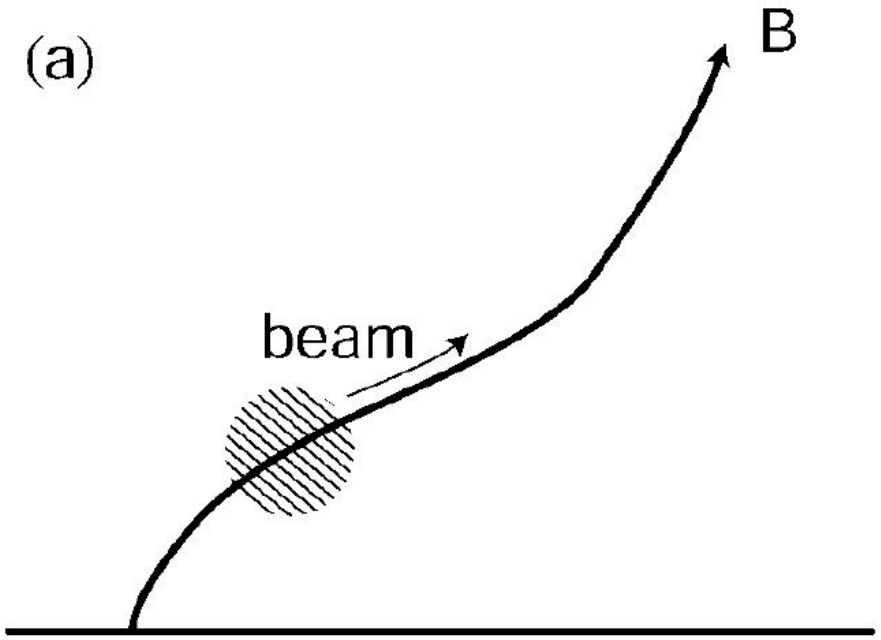

Normal

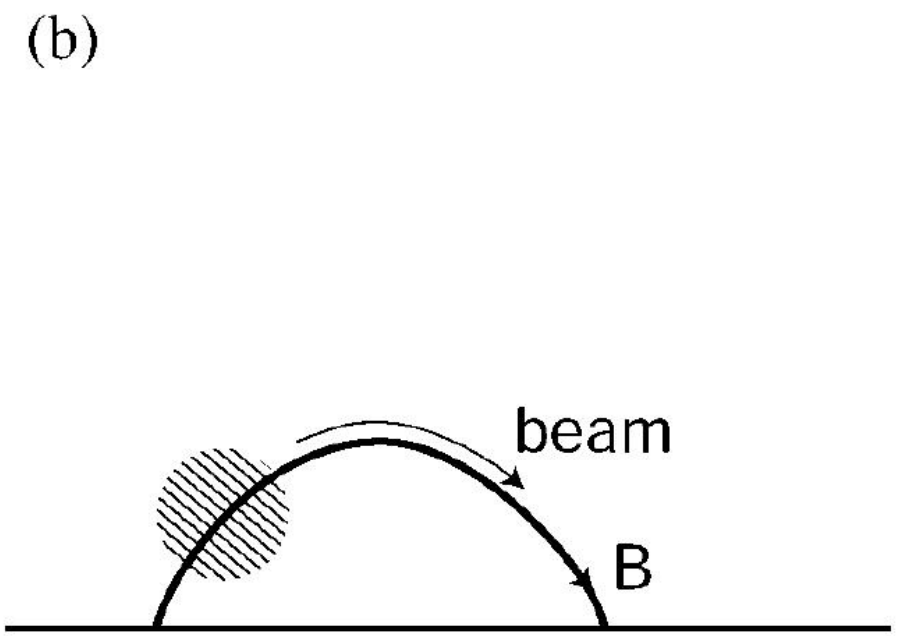

Invert-U or J

MorophologiesType III solar radio burst

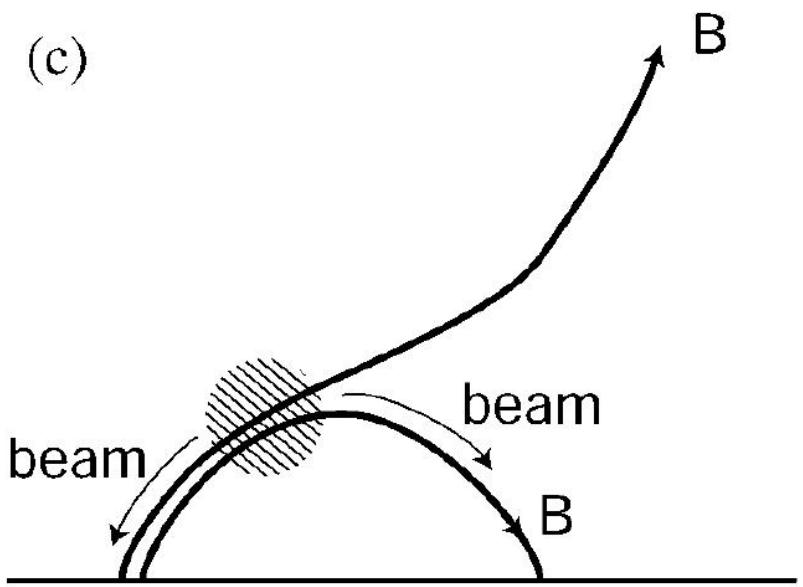

reverse-slope

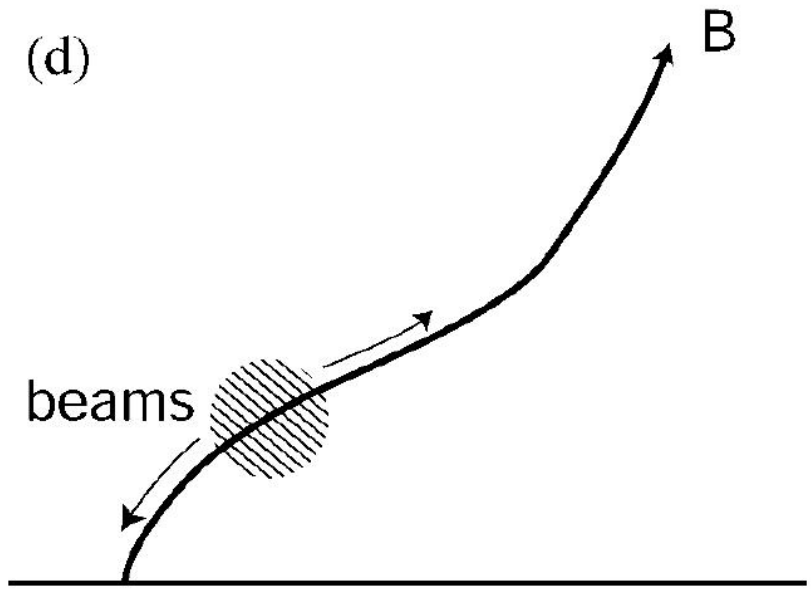

bidirectional(type III pair)

Schematic diagram of the background conditions of type III bidirectional burst(from Tan 2016)

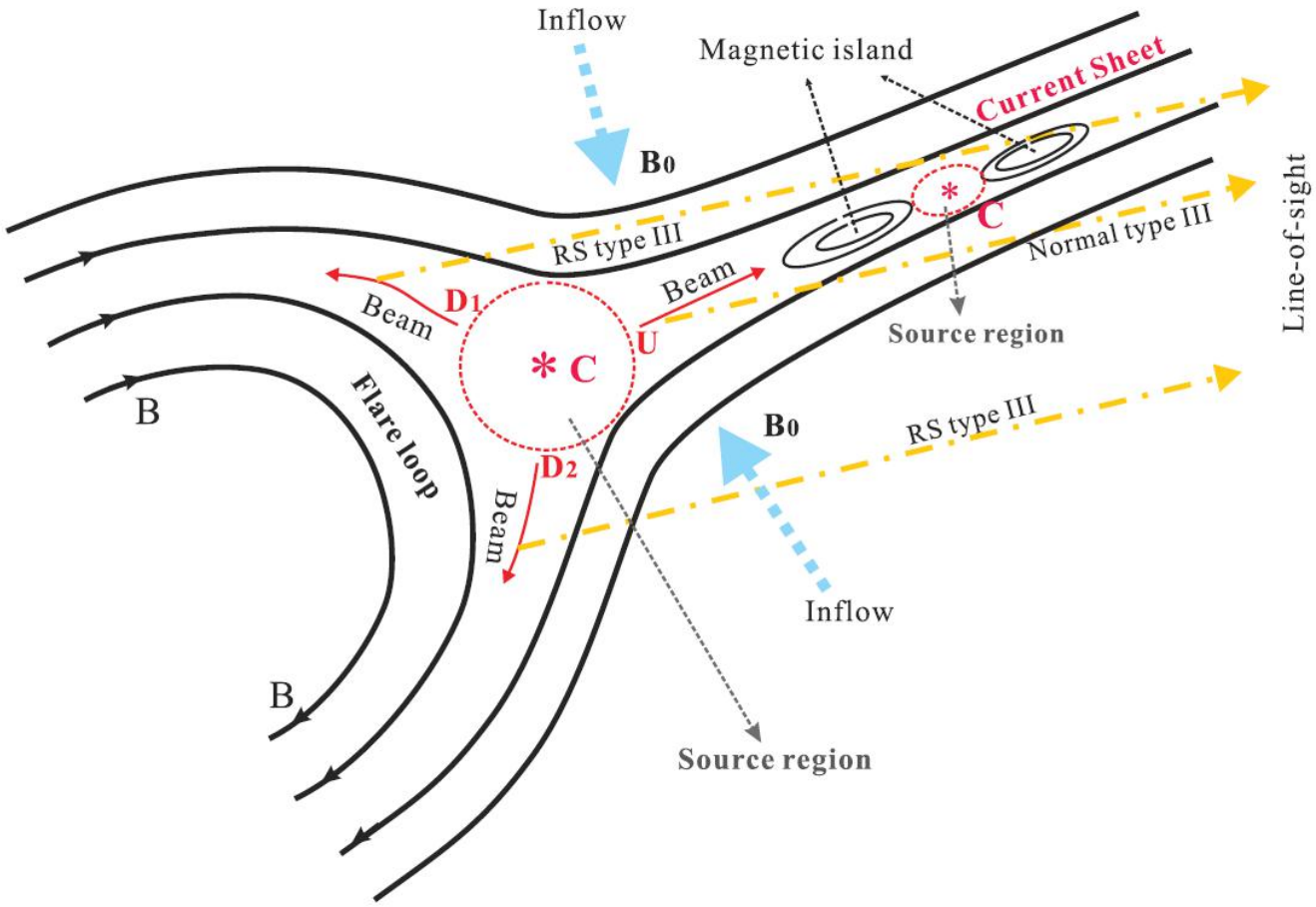

Observation of Radio Spectrometer

2014/04/04 C8.4 Flare
From Ondˇrejov
radiospectrograph
in the Czech Republic
(ORSC)

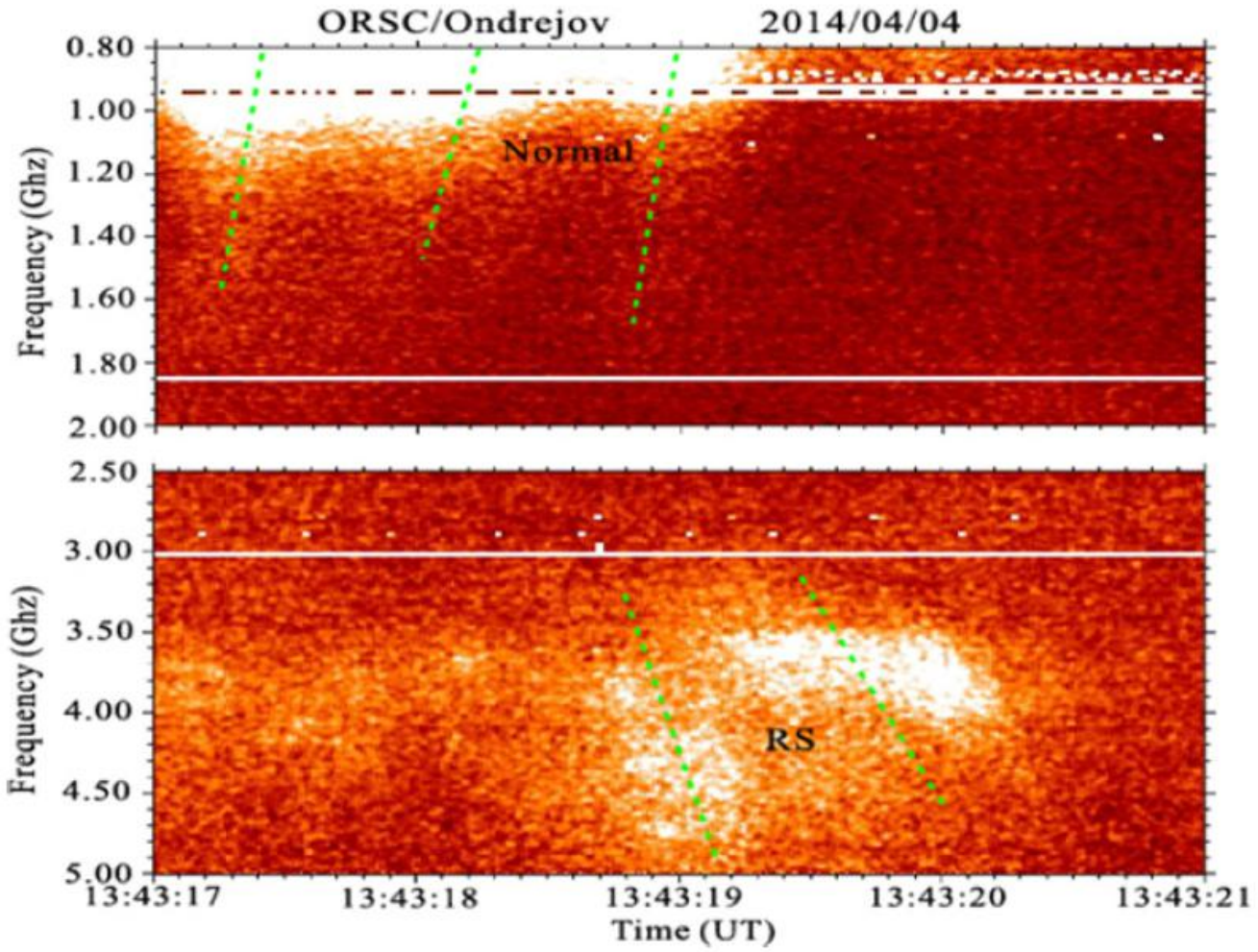

Observation of Radio Spectrometer

2011/09/26
From Ondˇrejov
radiospectrograph
in the Czech Republic
(ORSC)

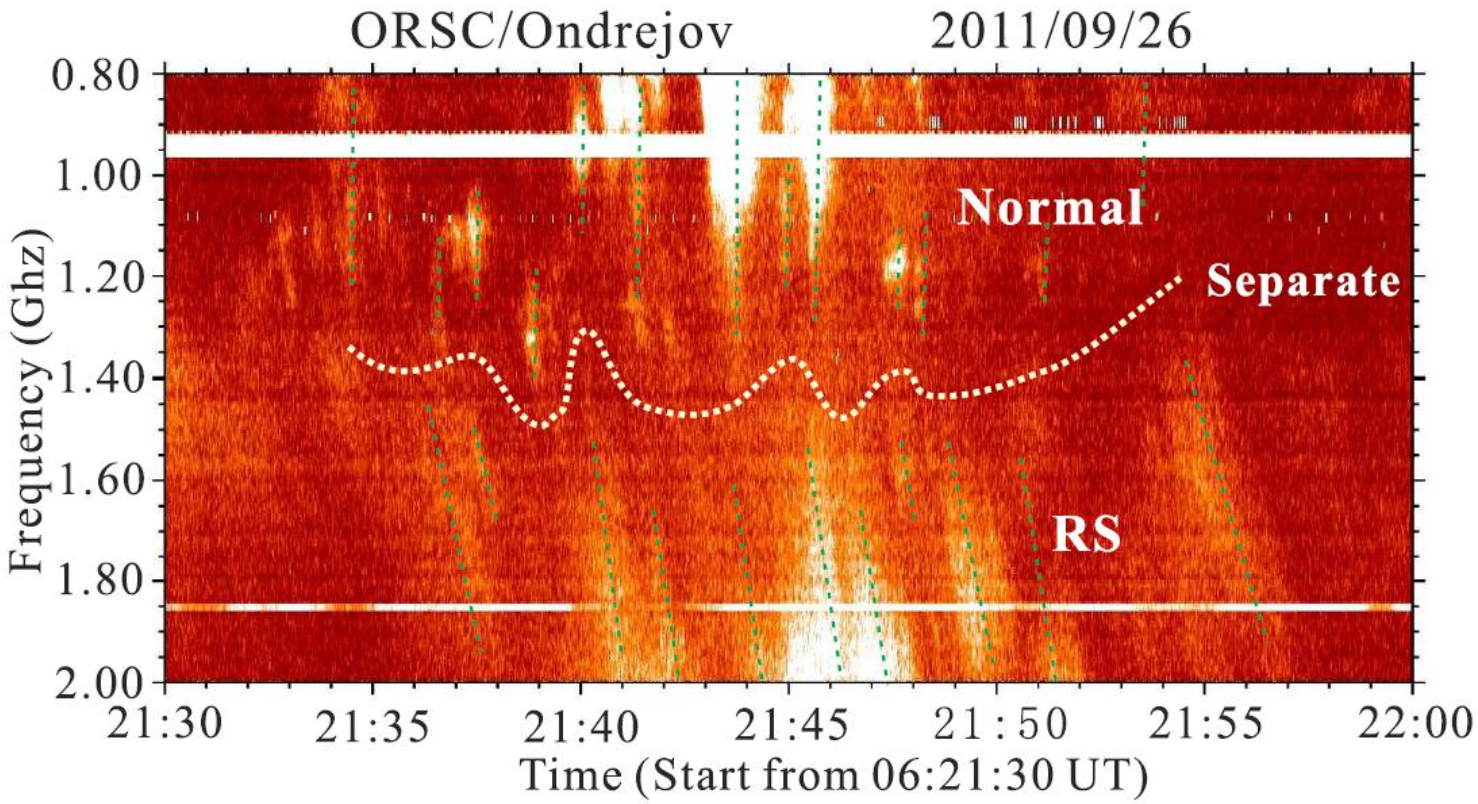

Observation of Radio Spectrometer

From the dynamic spectrum in last slide, we can get that the frequency drift(defined as the slope in the spectrograms D = df/dt) of the normal branches(about 2.12-7.38Ghz/s) is larger than the RS branches(about 281~647Mhz/s) in one order of magnitude.

Define the seperate frequency as the boundary frequency between the different branches. Here the line is nearly the middle of the frequency gap.

Possibly weak polarization, likely to be the second harmonic plasma emission.

Hard X-Ray Observation in 2011/09/26

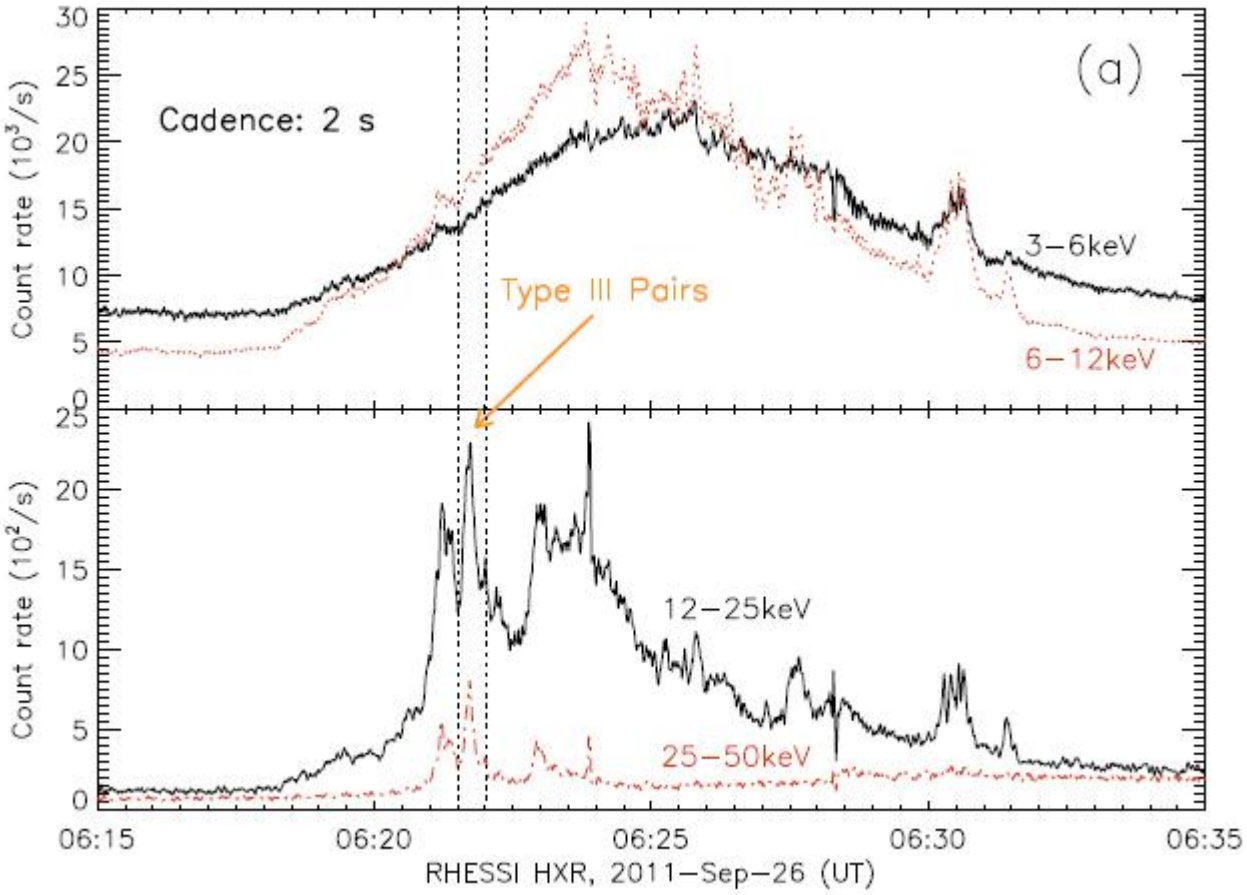

RHESSI HXR light curve
We can see the low energy X-ray is smooth during the Type III burst timerange but the high energy HXR have sharp splikes and one of it is just during that Type III timerange

Hard X-Ray Observation in 2011/09/26

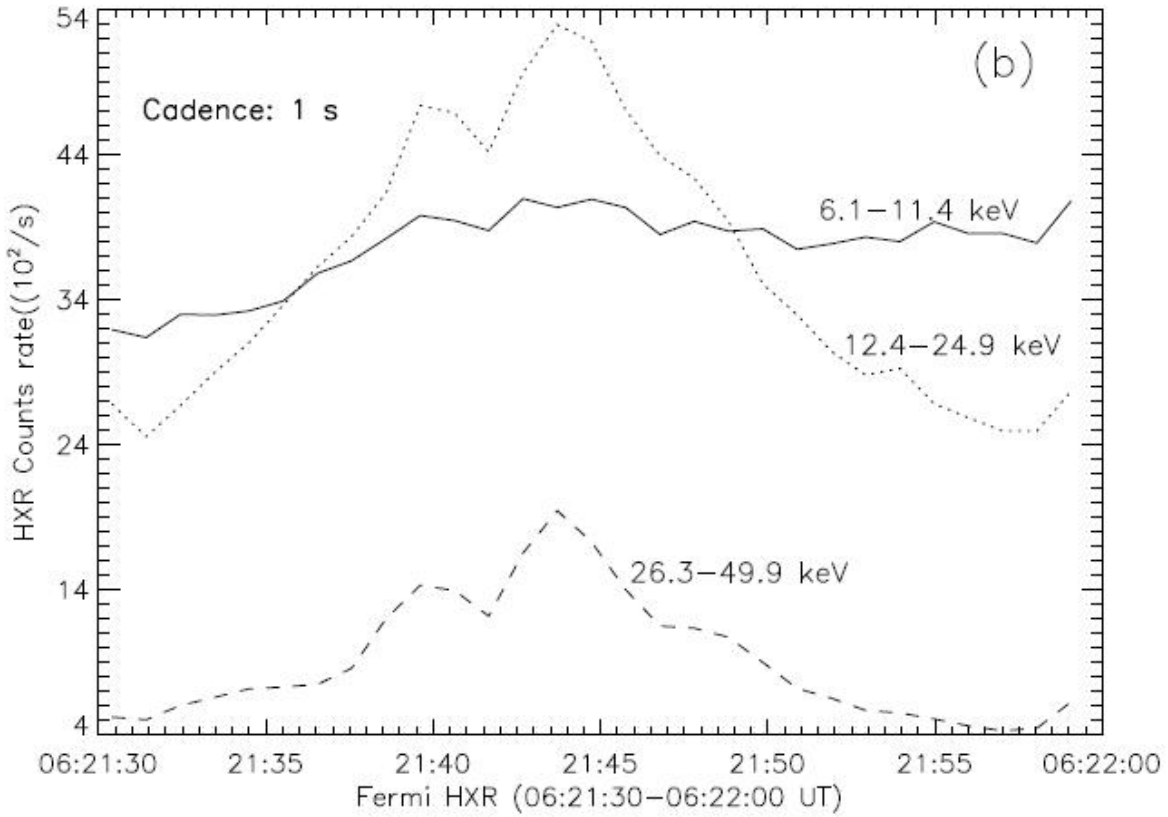

The curve from GBM
It shows that this bidirectional type III burst is more likely to closely related to enhancements of nonthermal HXR emission at energy of 12.4-24.9 and 26.3-49.9keV.

Hard X-Ray Observation in 2011/09/26

The bidirectional type III burst is at the impulsive rising phase of X-ray emission at energy of 3-12keV and coincided with a sharp HXR spike at non-thermal HXR at energy above 12keV. It may imply that the type III burst will share the same population with the nonthermal electrons which generated the HXR burst.

Imaging Observation of the Source Region

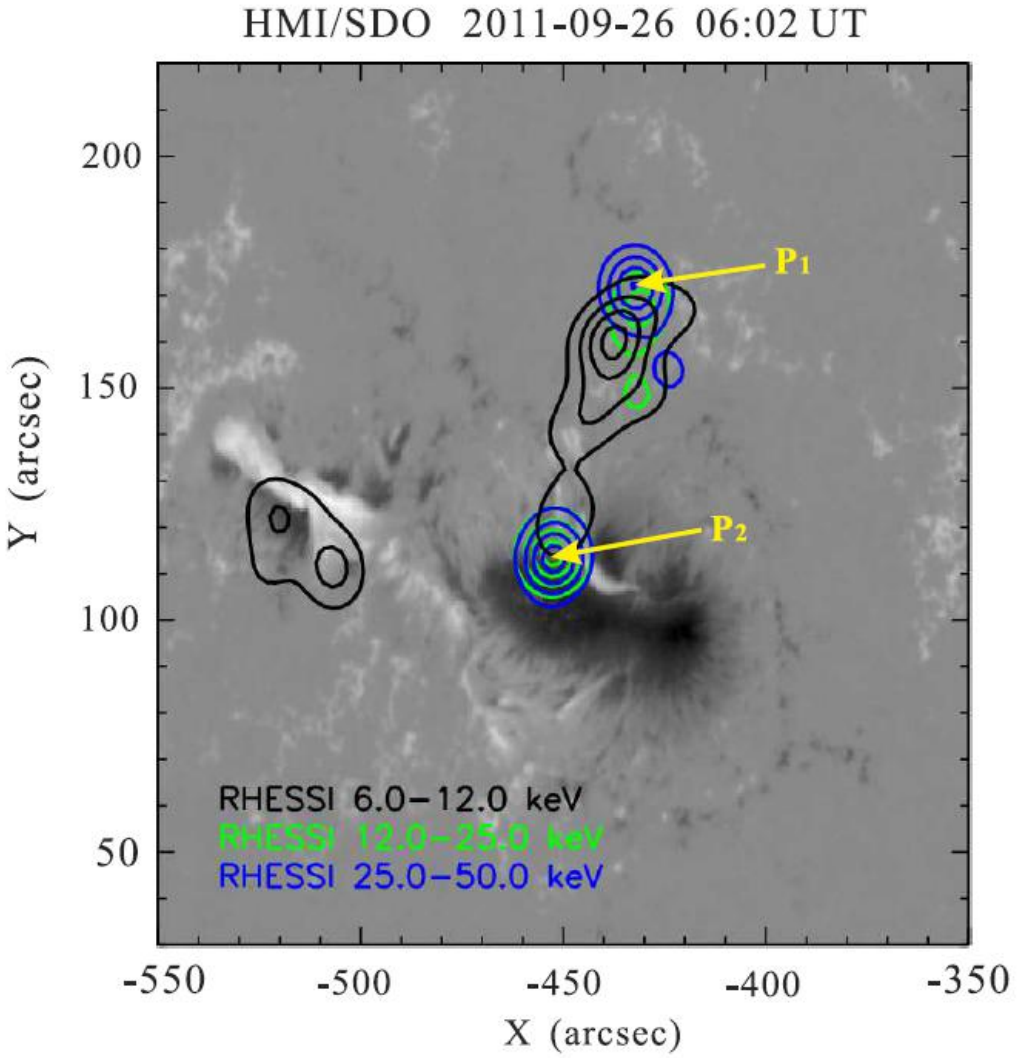

The two SXR maxima of 6-12keV overlayed on two regions with same magnetic polarity while the HXR maximaare overlaying the the regions with two opposite magnetic polarities. Possibly that two point are very close to the footpoints of flare loop.

Imaging Observation of the Source Region

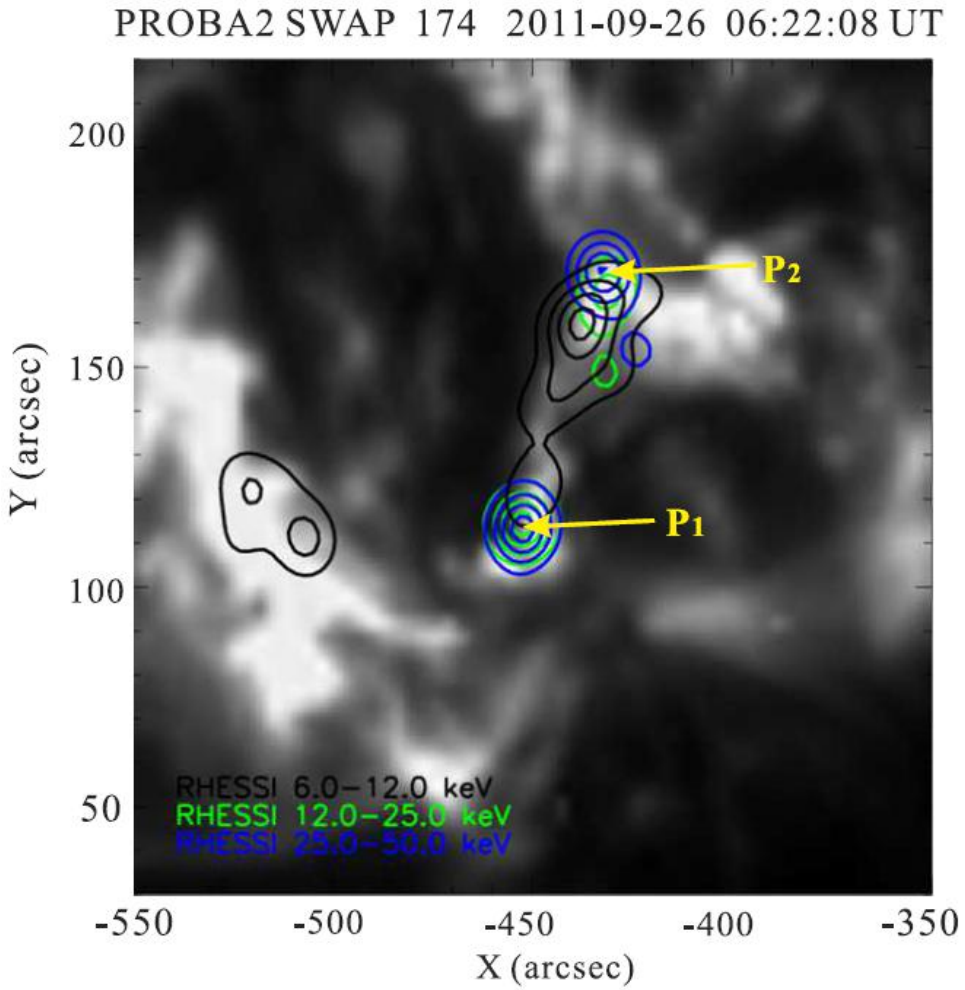

From a serious of SWAP EUV images, it shows a small enhancement near P2 during the type III burst time. This imply that the downward energetic electron beams associated to the
RS type III bursts may contribute to heating the underlying plasmas near the footpoints of the flaring loop.

Then we follow the diagnostics step of source region

The plasma density and magnetic field near the emission start sites of type III bursts:

$$n_e = f_{st}^2/81s^2 \ (m^{-3}),$$

$$B_L < B < B_H$$

In first equation, s is harmonic number, and f_{st} is the observed start frequency, this is from the relationship betwen emission frequency and plasma dynesity in plasma emission mechanism. In second condition,

$$B_L = 3.402 \times 10^{-19}(n_e T \bar{D} R_c)^{\frac{1}{2}} \qquad B_H = 3.293 \times 10^{-16}[\frac{n_e T \bar{D} R_c}{(n_e \tau)^{\frac{1}{3}}}]^{\frac{1}{2}}$$

These two are the lower and upper limits of magnetic field. Rc is the curvature radius expressing the divergence of magnetic field lines, T is the plasma electron temperature. The average of BL and BH can be regarded as the best estimator of magnetic field: B ~ 1/2 (BL + BH).

Then we follow the diagnostics step of source region

Then is about the velocity of the energetic electrons:

$$v_b \approx \frac{2\mu_0 n_e k_B T}{B^2} \bar{D} R_c,$$

and then we can get the energy of the nonthermal electrons (unit in keV)

$$E \approx 256 \frac{(v_b/c)^2}{\sqrt{1-(v_b/c)^2}}$$

the equation above indicates that the beam velocity is dominated not only by the relative frequency drift rate, but also by the magnetic field strength near the emission source region. Here, the velocity is proportional to the relative frequency drift rate, and inverse proportional to the square of magnetic field.

Then we follow the diagnostics step of source region

Then with the results above, we can get the plasma $\beta = \frac{n_{st} k_B T}{B^2/(2\mu_0)}$ and density scale length $H \approx \beta R_c / 2$, then we estimate the distance from the acceleration site to the emission start site, it can be regarded as the acceleration length (Lc), it is also the scale size of the source region.

$$L_c \approx H \cdot \frac{\delta f}{2 f_{st}}.$$

One thing worth to note that there are two kinds of reconnection sites, one is located in the cusp configuration near the loop top, the other is in the current sheet above the flare loops. As the current sheet may trigger the tearing-mode instability and produce the quasi-periodic pulsating structures in the microwave bursts (Kliem et al. 2000). In this work the type III pair train has no such pulsating property, therefore the author tend to suppose the reconnection site is possibly located in the cusp configuration.

Diagnostic Results

Apply the model to both the normal branch(with subtitle 'n') and the RS branch(with suntitle'r') . Then we may estimatethe physical conditions near the source region.

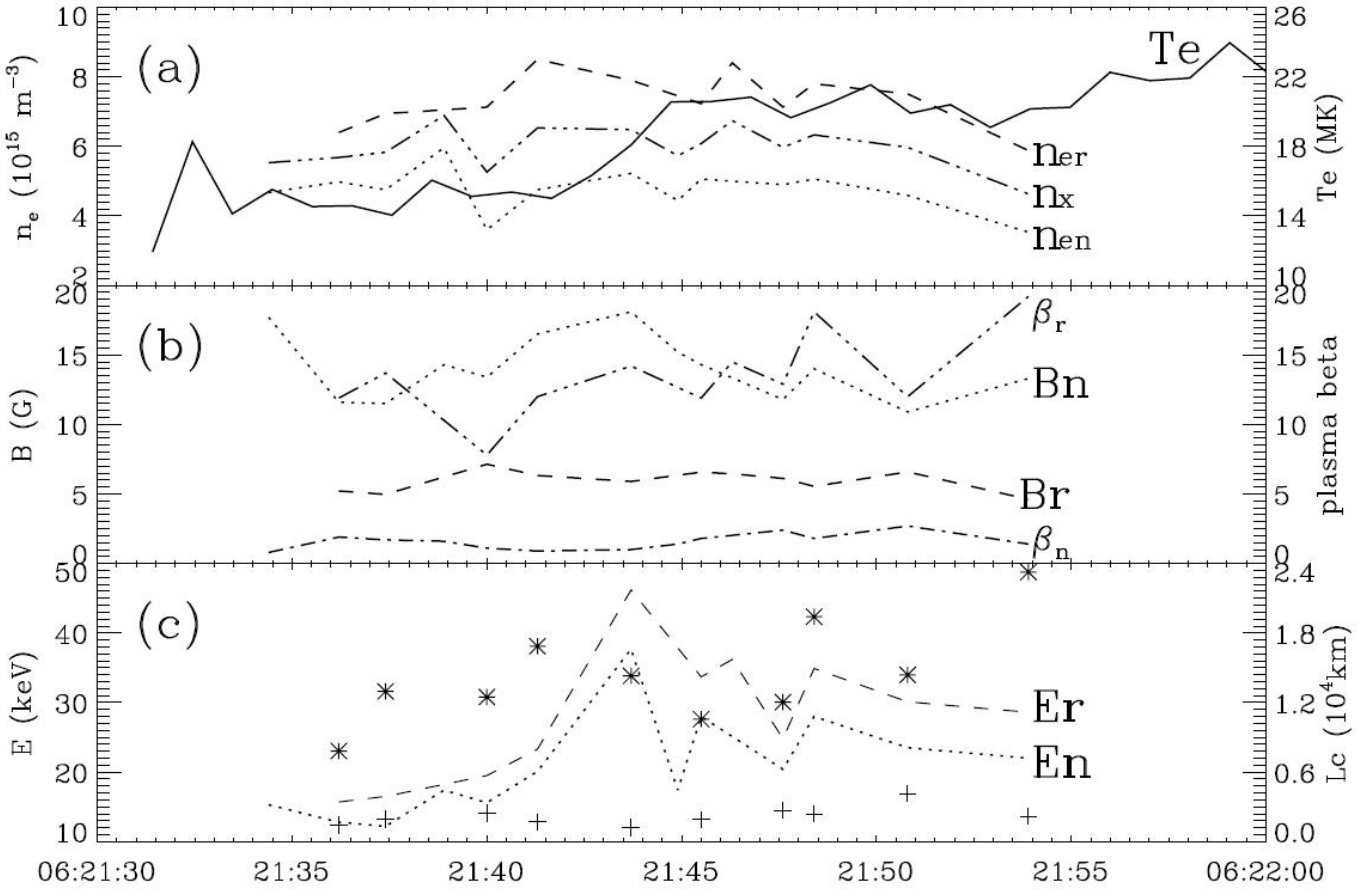

Evolution of physical conditions around type III burst

Diagnostic Results

In panal a,Here, the plasma temperature is derived from the X-ray emission observed by GBM/Fermi with cadence of about 1 s The background is subtracted as a values of non-flare periods. The model consists of thermal function (the optically thin thermal bremsstrahlung radiation function for one temperature) and a thick target model in power-law function. The derived temperatures are in a range of 12 - 24 MK during the microwave type III pair train (the black solid curve).

The plasma densities near the emission start sites of the normal and RS type III bursts are over-plotted in dotted and dashed curves. The density near the start sites of the normal type III bursts is in a range of (3.5 - 6.0)×10^15m^−3, and (5.9 - 8.5)×10^15m−^3 near the start site of RS type III bursts. We may derive the plasma density near the electron acceleration site (nx) which is the middle between the above two values, that is around 6×10^15m^−3 with little variations .

Diagnostic Results

In panal b, the derived magnetic fields near the emission start sites of the type III bursts are showed. It is interesting that the magnetic field near the start site of the RS type III branches is in a range of 4 - 8 Gauss, weaker than that near the start site of the normal type III branches (9 - 18 Gauss). And usually the coronal magnetic field is decreasing with the height. The possible explaination is that in magnetic reconnection regime, the anti-paralleled component of magnetic field near the reconnection site is very close to 0 where is a magnetic singular point and electron acceleration takes place around it (the other place is in the center of current sheet where the magnetic field tends to be near 0). The magnetic field increases from the reconnection site to the emission start sites of microwave type III burst (U, D1 and D2), which is obviously different from the general coronal magnetic field.

Diagnostic Results

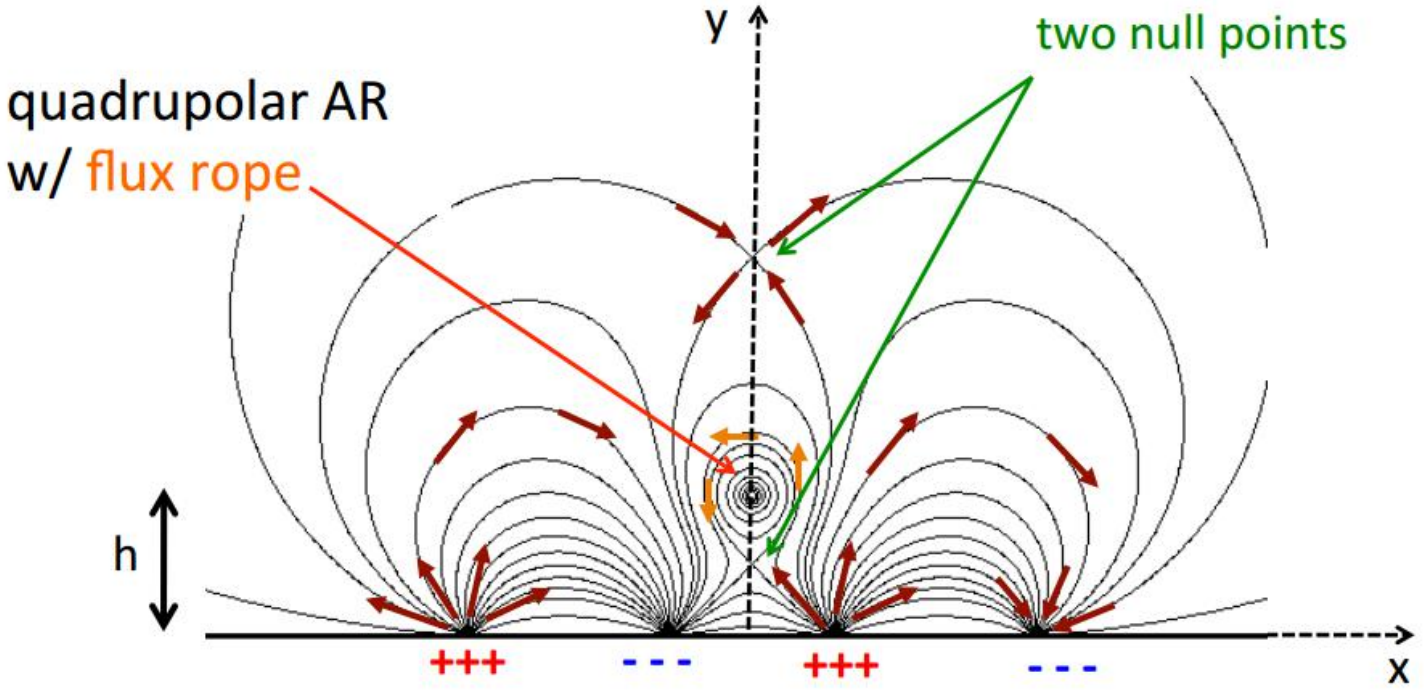

A toy model from Longcope

Diagnostic Results

In panal c, The velocities of the upgoing energetic electrons are in a range of 0.22 - 0.37 c, a bit smaller than that of the downgoing energetic electrons (0.24 - 0.41 c). The corresponding energies are 12 - 38 keV and 16 - 47 keV for the upward and downward electron beams, respectively. Here, we find that although the RS type III branches drift much slower at about one order of magnitude than the normal type III branches, but the corresponding energy difference of the downgoing and upgoing electrons is only from 2.7 keV to 9.5 keV, which is relatively very small.

With such great different drift rates, we still obtained similar energies of the upgoing and downgoing electrons. The reason is that although the relative drift rates between the two branches have an order of magnitude apart, but their magnetic field strengths also have several times apart, and these make it is possible to yield similar beam velocities.

The little difference between the upgoing and downgoing electrons indicates that they may accelerate possibly by the similar mechanism and more effective to the downgoing electrons in the magnetic reconnection region.

Diagnostic Results

Also the author mention the plasma beta, In this work β_p are in range of of 0.8 - 2.6 and 7.5 - 18.5 in the start sites of the upgoing and downgoing electron beams. The large value implies the more violent instability in the magnetized plasma. The particle acceleration may be more effective to the downgoing electrons than to the upgoing electrons in the flare impulsive phase.

The author make an estimation of the scale size of acceleration region (Lc) which is in a range of (1.2 - 4.1)×10^3 km (the plus signs + in panel c) for the upgoing electron beams and (0.8 - 2.3)×10^4 km for the downgoing electron beams (the star sigh ∗ in panel c). This means that type III bursts begin to generate just after the energetic electron beam propagating a considerable distance from the acceleration site.

Discussion and Summary

Then the author get few properties from the results:
(1) The plasma density associated to the start site of RS type III branches is higher than that of normal type III branches, while the magnetic field associated to the emission start site of RS type III branches is weaker than that of normal branches, and these lead to the plasma beta values near the start site of RS type III branches higher than that of the normal branches.
(2) Although the RS type III branches drift slower at about one order of magnitude than the normal type III branches, the energies of the downward electron beams are still very close to that of the upward electron beams.
(3) The plasma density, temperature, magnetic field strength, and the distance between the acceleration and the emission start sites almost have no obvious variations during the period of type III pair trains, while the derived energy of electrons has an obvious peak value which is consistent to the hard X-ray emission during the half minute of type III pair burst.

Discussion and Summary

According to these facts, the author imply both of the upgoing and downgoing electron beams are accelerated by similar mechanism in the magnetic reconnection region, and their little difference is just because of their different background conditions, including the plasma density, magnetic field strength and the scale size of the source region, etc.

The above calculations indicate that most of the plasma beta near the emission start sites of microwave type III pair bursts are around or even greatly higher than an unity. This fact may reflects the highly-dynamic properties of the source region where magnetic reconnection and particle accelerations (by the reconnecting electric field) take place.

Discussion and Summary

Several points need more discussion:
Actually, the magnetic field tend to be very weak and the plasma beta may become very large near the reconnecting site. Around these sites, not only the magnetic reconnection and electron acceleration take place, but also the plasma turbulence and various plasma instabilities occur.Therefore it is much different and complicated from the plasma in the coronal background and flaring loops.
And the figure bofore shows that the upward electron beams may meet the magnetic islands in the current sheet, and here the magnetic curvature radius Rcn will possibly become smaller than the radius of the flare loop. We adopt the flare loop to approximate Rc in both normal and RS type III burst regimes, this will overestimate Rc and the magnetic field near the start site of the upward beams, and underestimate the plasma beta. Equation before indicates $vb \propto RcB{-}2$ which may derive that the velocity (vb) is independent to the magnetic field strength. So, the uncertainties of magnetic field will not affect the estimation of the velocity and energy of the electrons.

Discussion and Summary

From the author's point, there are still uncertainties in estimating the magnetic field near the emission start site of the normal type III branches. Equation before indicates that magnetic field estimation (B) depends on the curvature radius Rc of the magnetic field ines. Rc for the normal type III branches should be different from that for RS type III branches. Figure 4 shows that the start sites (U) of the upward electron beam locate above the magnetic reconnecting site (C) and the start sites (D1 and D2) of downward electron beam locate below the magnetic reconnecting site. D1 and D2 are very close to the top of flare loop while U is close to the current sheet above the flare loop. In current sheet, the tearing-mode instabilities may take place and produce magnetic islands and plasmoids which can result in the complex magnetic structures. Therefore, the Rc of the magnetic field lines near the site of U may be different to that near D1 and D2.. As an expedient, the author simply use the flare loop radius to approximate it.

Thanks for listening